Video Article

Unraveling Key Players of Humoral Immunity: Advanced and Optimized Lymphocyte Isolation Protocol from Murine Peyer's Patches

Yavuz F. Yazicioglu[1,2], Halil I. Aksoylar[1,2], Rinku Pal[1,2], Nikolaos Patsoukis[1,2], Vassiliki A. Boussiotis[1,2]

[1]Division of Hematology-Oncology, Beth Israel Deaconess Medical Center, Harvard Medical School

[2]Department of Medicine, Beth Israel Deaconess Medical Center, Harvard Medical School

Correspondence to: Vassiliki A. Boussiotis at vboussio@bidmc.harvard.edu

URL: https://www.jove.com/video/58490
DOI: doi:10.3791/58490

Keywords: Cancer Research, Issue 141, Peyer's patches, follicular T helper cells, germinal center B cell, lymphocyte isolation, tissue preparation, lymphocyte subsets, lymphoid organs, collagenase

Date Published: 11/21/2018

Citation: Yazicioglu, Y.F., Aksoylar, H.I., Pal, R., Patsoukis, N., Boussiotis, V.A. Unraveling Key Players of Humoral Immunity: Advanced and Optimized Lymphocyte Isolation Protocol from Murine Peyer's Patches. *J. Vis. Exp.* (141), e58490, doi:10.3791/58490 (2018).

Abstract

In the gut mucosa, immune cells constitute a unique immunological entity, which promotes immune tolerance while concurrently conferring immune defense against pathogens. It is well established that Peyer's patches (PPs) have an essential role in the mucosal immune network by hosting several effector T and B cell subsets. A certain fraction of these effector cells, follicular T helper (TFH) and germinal center (GC) B cells are professionalized in the regulation of humoral immunity. Hence, the characterization of these cell subsets within PPs in terms of their differentiation program and functional properties can provide important information about mucosal immunity. To this end, an easily applicable, efficient and reproducible method of lymphocyte isolation from PPs would be valuable to researchers. In this study, we aimed to generate an effective method to isolate lymphocytes from mouse PPs with high cell yield. Our approach revealed that initial tissue processing such as the use of digestive reagents and tissue agitation, as well as cell staining conditions and selection of antibody panels, have great influence on the quality and identity of the isolated lymphocytes and on experimental outcomes.

Here, we describe a protocol enabling researchers to efficiently isolate lymphocyte populations from PPs allowing reproducible flow cytometry-based assessment of T and B cell subsets primarily focusing on TFH and GC B cell subsets.

Video Link

The video component of this article can be found at https://www.jove.com/video/58490/

Introduction

The entire gastrointestinal tract from the beginning to the end is decked with an extensive lymphoid network that contains immune cells more than any other organ in human and mouse[1]. Peyer's patches (PPs) constitute a major component of the intestinal branch of this cellular immune organization, so-called gut-associated lymphoid tissue (GALT)[2,3]. Within PPs, thousands of millions of antigens derived from dietary materials, commensal microbiota and pathogens are being sampled continuously, and when necessary appropriate immune responses toward them are mounted thus maintaining intestinal immune homeostasis. In that sense, PPs could be named as "tonsils of the small intestine". PPs consist of major sub-compartments: subepithelial dome (SED), large B-cell follicle zones; the overlying follicle-associated epithelium (FAE) and interfollicular region (IFR) where T cells are located[4]. This unique compartmentalization of PPs enables different effector cell subsets to cooperate, thus, confers immunocompetence in the gut.

PPs lack afferent lymphatics, and due to this reason, antigens transported to PPs from small intestine are not being conducted through lymphatic vessels in contrast to most of the other lymphoid organs. Instead, specialized epithelial cells located in FAE, so-called M cells, are responsible for the transfer of luminal antigens into the PPs[5]. Subsequently, the transported antigens are picked up by the dendritic cells (DCs) and phagocytes that are located in the subepithelial dome (SED) region beneath the FAE[6,7]. This antigen sorting process by DCs in the PP is crucial to initiate adaptive immune response[8] and subsequent generation of IgA secreting cells[9].

Due to the heavy antigenic burden from commensal flora and dietary material, PPs host endogenously activated effector T and B cell subsets in great abundances such as TFH and IgA^+ GC B cells[10], suggesting that PPs represent a site of active immune response[11]. Detection of up to 20–25% TFH cells within total $CD4^+$ T cell compartment and up to 10–15% GC B cells within total B cells is possible in PPs collected from unimmunized young C57BL/6 mice[12]. In contrast to other T helper cell types (*i.e.*, Th1, Th2, Th17 cells), TFH cells show unique tropism into B cell follicles primarily owing to CXCR5 expression, which promotes TFH cell homing along CXCL13 gradient[13]. In the B cell follicle zones of PPs, TFH cells induce IgA class switch recombination and somatic hypermutation in activated B cells from which high-affinity IgA producing cells differentiate[14]. Subsequently, these antibody-secreting plasma cells migrate to the lamina propria (LP) and regulate immune homeostasis in the gut[10].

Identification and characterization of TFH and GC B cell populations within PPs might enable researchers to investigate the dynamics of humoral immune responses under steady-state conditions without the need of time-consuming immunization models traditionally used in TFH-GC B cell studies[15,16,17,18]. Analyzing TFH cells within PPs is not as straightforward as other cell subsets. Technical challenges include identifying ideal tissue preparation conditions, surface antibody-marker combination, as well as selecting appropriate positive and negative controls. Both TFH and PP research fields exhibit great variability in terms of experimental procedures and are far from conferring a consensus to establish standardized protocols due to several reasons. First, each cell subset within PPs tends to be affected differentially by tissue preparation conditions requiring further modifications in a cell subset-specific manner. Second, there is a significant discrepancy among the reported methods regarding the details of cell preparation from PPs. Third, the number of protocol-based comparative studies investigating ideal tissue preparation techniques and experimental conditions for PP and TFH research is rather limited.

Current protocol-based studies suggested for PP cell preparation[19,20,21,22] were not TFH- or GC B cell-oriented. Moreover, some tissue preparation conditions recommended for PPs[19,20] such as collagenase-based digestion were found to affect the outcome of TFH identification by flow cytometry negatively[18]. On this basis, we reasoned that an optimized, standardized and reproducible protocol that can be used to study TFH and GC B cell dynamics within PPs would be valuable to investigators working on this topic. This need gave us the impetus to generate an improved and up-to-date protocol for the isolation and characterization of PP lymphocytes that is finely optimized for cellular recovery, viability, and efficiency for flow cytometric characterization of several T and B cell subsets. We also aimed to exclude several laborious preparation steps suggested in previous protocols, thereby, reducing the required manipulations and time for tissue and cell preparation from PPs.

Protocol

All studies and experiments described in this protocol were conducted under guidelines according to Institutional Animal Care and Use Committee (IACUC) of Beth Israel Deaconess Medical Center.

1. Designing Experimental Set-up and Mouse Groups

1. (Optional) Co-house the experimental mice to facilitate horizontal transmission of gut microbiota between experimental mice and to reduce non-specific variability within PP lymphocytes. Additionally, use littermate controls of the same gender to minimize variability.

2. Surgical Excision and Tissue Preparation Steps:

1. Surgical removal of the Small Intestine (SI)
    1. Euthanize mice using CO_2 asphyxiation or any equivalent method approved by the institutional animal ethics committee.
    2. Transfer the mouse to a dedicated area for surgical excision. Place backside down and sanitize the abdomen with 70% ethanol. Perform a laparotomy by cutting the abdominal skin and peritoneum along the midline from pubis to the rib cage thus opening the peritoneal cavity.
    NOTE: Perform the first incision on a relatively small area of the skin to avoid penetrating the peritoneal cavity and damaging intestinal tissue. Continue the excision until desired anatomical border.
    3. Identify the caecum, which is an ideal landmark for the detection of the terminal ileum, which constitutes the distal segment of the small intestine.
    NOTE: Caecum is usually located on the lower left side of the mouse abdomen.
    4. Pinpoint ileocaecal junction and make a cut at this level as distal as possible to separate the small intestine from the caecum. Throughout the next steps, avoid excessive physical contact with the intestinal wall because fragile PPs collapse easily upon touch.
    5. Gently remove the entire small intestine until the pyloric sphincter by cutting the mesentery using scissors. Identify the junction between pylorus and duodenum, and snip the duodenum at this level, which will lead to complete detachment of small intestine from the abdominal cavity.
    NOTE: (i) Avoid hyperextension as this might cause the rupture of the intestinal wall**. (ii)** If LP lymphocyte isolation is desired in addition to PP lymphocytes, complete removal of the mesenteric fat is necessary. However, for PP isolation only, remaining mesenteric fat could provide some benefits during the further isolation steps; therefore, it should be preserved.
    6. Place detached small intestines in a 6-well plate filled with cold RPMI + 10% fetal bovine serum (FBS) and gently agitate the tissues manually until all intestinal segments are submerged in the cold media. Maintain the tissues on ice throughout the next steps.
    7. After dissecting the desired number of mouse small intestines, proceed to PP excision from collected small intestines.

2. Surgical Excision of PPs and Preparation of Single Cell Suspension:
    1. Gently transfer the small intestine on a paper towel by gripping the mesenteric fat using forceps and place the mesenteric side facing the paper towel. Moisten the entire intestinal segment with cold RPMI + 10% FBS to avoid tissue dehydration and stickiness.
    NOTE: Remaining mesenteric fat can be helpful at this stage because fat tissue segments on the mesenteric site of SI will stick to the paper towel keeping the anti-mesenteric site facing up.
    2. Identify the PPs, which appear as white multi-lobulated aggregates in a “cauliflower-like” shape on the anti-mesenteric side of the intestinal wall.
    NOTE: Flushing out the luminal content is not recommended until all PPs are excised. Emptying the luminal content might cause the collapse of the PPs and will prevent the color contrast between PPs and the intestinal wall, which is very helpful for visual identification of PPs.
    3. After identifying PPs on the anti-mesenteric side, place the surgical curved-end scissor on PPs (curve should face up) restraining the PP from its distal and proximal border.
    Optional: Push the PP gently toward the blades of scissor using a fingertip. This maneuver will lead to the better exclusion of surrounding non-PP tissue. Excise the PPs gently, excluding the surrounding intestinal tissue.
    NOTE: (i) This step is crucial to obtain maximal PP cell yield while minimizing the cell contamination from neighboring intestinal compartments such as LP and intestinal epithelium, which are also rich in T cells. (ii) From one SI excised from C57BL/6 mouse, 5-10

PPs (average size, multi-lobulated) can be collected. By aiming even smaller PPs (not multi-lobulated), collection of up to 12-13 PPs per mouse (C57BL/6) is possible using this protocol.

4. Transfer the excised PPs to a 12-well tissue culture plate filled with ice-cold RPMI + 10% FBS and maintained on ice using forceps or curved surgical scissors.
   NOTE: (i) Immediately after excision of PPs, mucus and intestinal content on the PP surface can be cleaned by rubbing the tissue gently on a paper towel. This step will help improve the viability of PP lymphocytes. (ii) Instead of transferring the PPs to a plate, transferring to separated tubes can also be considered depending on total sample number.
5. Optional: When PP excision and subsequent placement into the well plate are completed, the number and size of PPs collected from different experimental/mouse groups can be documented by taking a picture of the tissue culture plate containing PPs.
6. Prepare a set of 50 mL conical tubes filled with 25 mL of RPMI + 10% FBS (pre-warmed at 37 °C). Using a pair of scissors, cut the edge of a 1,000 µL tip from the distance that will allow the aspiration of the PPs with 1 mL pipette. Aspirate the PPs with 1 mL pipette and transfer them from the 12-well tissue culture plate to the prepared 50 mL conical tubes.
   NOTE: Use a new tip for each mouse sample to avoid cross-contamination among the samples.
7. Secure the lid and place the tubes vertically in an orbital shaker at 37 °C, with continuous agitation at 125–150 rpm for 10 min. Meanwhile, prepare a new set of 50 mL tubes and place a 40 µm cell strainer on the top of each tube, through which single cell suspension will be prepared.
   NOTE: (i) The agitation step will remove the remaining intestinal content, mucus and cell debris, which decrease the cell viability and recovery of PP lymphocytes if not removed. (ii) Do not apply any kind of digestive enzymes on PP tissue because the digestion process causes a dramatic loss of CXCR5 expression from the cell surface.
8. After the agitation, transfer the PPs to the 40 µm cell strainer placed on the top of the newly prepared conical 50 mL tubes. Using the rounded side of a 10 mL syringe plunger, gently disrupt the PPs through the cell strainer to generate single cell suspension. Rinse the strainer with 15–20 mL of cold RPMI + 10 % FBS.
   NOTE: (i) Before filtering, shake the tubes containing the PPs horizontally. This short shake will facilitate the transfer of PPs into cell strainers. (ii) Using a 70 µm cell strainer for the isolation of non-lymphoid immune cells (*e.g.*, monocytes, macrophages, DCs) is recommended.
9. Centrifuge the single cell suspensions at 350–400 x g for 10 min at 4 °C.
10. Carefully discard the supernatant and resuspend the cells at a concentration of 10 x 10^6 cells/mL. Count the cells using a hemocytometer.
    NOTE: (i) Prior to cell counting, the total cell number for each mouse PP group can be approximately estimated using the following formula: "0.5-1 x 10^6 cells x (number of PPs) = total cell count". Further dilutions with trypan blue for cell counting might be necessary. (ii) As an alternative to manual counting, automated cell counters can be used.
11. Transfer 2-2.5 x 10^6 cells in appropriate volume (*e.g.*, 200 µL) into a 96-well round-bottom plate.
    NOTE: For single color and negative control samples, 0.5-1 x 10^6 cells might be sufficient.
12. Centrifuge the plate at 350 x g for 5 min at 4 °C. Flick the plate.
13. Wash the cells in 200 µL of Staining Buffer.

3. Surface Antibody Staining

1. Viability Staining:
   1. After the final wash, resuspend the cells in 100 µL of fixable viability dye diluted in PBS (1:1,000). Incubate for 30 min on ice or at 4 °C in the dark.
      NOTE: (i) Intracellular staining for the detection of key transcription factors such as Foxp3 or Bcl-6 requires fixation of the cells. In that case, non-fixable viability dyes (*e.g.,* 7-AAD, DAPI) cannot be used. (ii) To dilute fixable viability dye, do not use any staining buffer that contains protein. The media used in this step must be protein-free. (iii) Exclusion of dead cells by using viability staining is crucial because dead cells can cause serious technical difficulties in flow cytometry analysis by emitting autofluorescence and by binding surface antibodies nonspecifically, which might lead to false positive results.
   2. Wash the cells twice with staining buffer. Centrifuge at 350 x g for 5 min at 4 °C. Flick the plate.

2. Fc Block and Surface -Layer I:
   1. Prepare the Fc-block solution by diluting anti-CD16/32 antibody (1:200) in staining buffer.
   2. Resuspend the cells in 20 µL of prepared Fc-block solution. Incubate for 15 min on ice.
   3. Without washing, add 80 µL of surface antibody cocktail (see **Table 1** for the antibody summary) prepared at appropriate dilutions. Incubate on ice for at least 30 min.
   4. Wash twice by adding excessive staining buffer. Centrifuge at 350 x g for 5 min at 4 °C. Flick the plate.

3. Surface -Layer II:
   1. Prepare Streptavidin staining solution by diluting fluorochrome-conjugated Streptavidin in staining buffer.
   2. After the final wash, resuspend the cells with 100 µL of pre-diluted Streptavidin (1:100) staining solution. Incubate for at least 15 min on ice in the dark.
   3. Wash twice with staining buffer. Centrifuge at 350 x g for 5 min at 4°C. Flick the plate.
      Optional: If intracellular staining for follicular regulatory T cell detection is not desired, after the last wash, resuspend the cells in 200 µL of staining buffer and transfer into appropriate tubes to acquire data in flow cytometer. When the samples are not fixed, acquisition of data by flow cytometry should be performed within 3–4 h to obtain accurate results.

4. Cell Fixation

1. Prepare fixation/permeabilization (Fix/Perm) working solution using the reagents from Foxp3/Transcription Factor Staining Buffer Set. Mix one-part of fixation/permeabilization concentrate with three parts of fixation/permeabilization diluent to the desired final volume.
2. After the final wash, resuspend the cells in 200 µL of Fix/Perm working solution.
3. Incubate the plate on ice or at 4 °C for 20 min. Do not exceed 20 min for this step. Longer incubation time might severely decrease the cell recovery.
4. Centrifuge at 350 x g for 5 min at 4 °C. Flick the plate. (**Optional**) After this step, fixed cells can be stored for several days at 4 °C in staining buffer containing bovine serum albumin (BSA) or FBS until subsequent intracellular staining or flow cytometry acquisition.
5. Resuspend the cells in 200 µL of permeabilization Buffer (x1) freshly pre-diluted in purified deionized water.
6. Centrifuge at 350 x g for 5 min at room temperature (RT).
7. Wash once with 200 µL of permeabilization buffer and centrifuge at 350 x g for 5 min at RT.

5. Intracellular Staining

1. Prepare the Fc-block solution by diluting anti-CD16/32 antibody (1:200) in permeabilization buffer.
   NOTE: After the fixation step, the cells must be maintained in permeabilization buffer until the end of the intracellular staining process.
2. After the final wash, resuspend the cells in 20 µL of Fc-block solution. Incubate for 10–15 min at RT in the dark.
3. Without washing, add 80 µL of intracellular antibody cocktail (100 µL final volume) pre-diluted in permeabilization buffer. Incubate for 30 min at RT.
4. Add 100 µL of Perm Buffer, and centrifuge at 350 x g for 5 min at RT.
5. Wash once with 200 µL of permeabilization buffer, centrifuge at 350 x g for 5 min at RT.
6. After the final wash, resuspend the cells in 200 µL of staining buffer and transfer the cells into appropriate tubes (final volume of 400 µL in staining buffer) and acquire data by flow cytometry. Samples stained in 96-well plate may also be run without transferring into tubes if a flow cytometer with plate reader option is available. This step minimizes cell loss during cell transferring.
7. Acquire a minimum of 5 x 10^5 total cells on the flow cytometer to be able to perform reproducible analysis of TFH, TFR as well as GC B cells.

Representative Results

In contrast to a previous protocol[20], we have observed that PPs are not evenly distributed throughout the SI but are localized more densely towards the distal and proximal ends of the SI as shown in **Figure 1A.** Flow cytometric analysis showed that, if followed correctly, our protocol gives a PP lymphocyte population that demonstrates forward-side scatter distribution similar to splenocytes (**Figure 2A, E,** and **2D, H**) with >95% cell viability (**Figure 2B** and **2F**). In contrast to other secondary lymphoid organs (SLOs), in C57BL/6 mice approximately 70–80% of total PP lymphocytes consist of B cells, whereas $CD4^+$ T cells constitute only 10–15% of total PP lymphocytes (**Figure 2C** and **2G**).

Please note that $CD4^+$ $CD19^+$ double positive (DP) cells constitute ≈ 1% of total PP lymphocytes. With certain precautions during cell preparation such as performing Fc-Block against Fc receptors of B cells and excluding doublets, $CD4^+$ $CD19^+$ DP cell population could be minimized (**Figure 3A** and **B**). However, a fraction of DPs that does not demonstrate forward scatter (FSC) characteristics of doublets is unavoidable and should be gated out from the single positive T and B cell gates (**Figure 3B**). Our results revealed that B cells within DP cells highly express CXCR5 on their surface (**Figure 3C**) that might lead to false positive results in the TFH gate which is adjusted based on CXCR5 expression in $CD4^+$ T cells. On the other hand, we found that GL7, a marker of activated B cells, is also expressed in $CD4^+$ $CD19^+$ DP cells (**Figure 3D),** which might cause interference with GC B cell gating.

Examples of TFH and GC B cell gating algorithms are depicted in **Figure 4.** For GC B cell gating, we use GL7 labeling versus CD38, which identifies GC B cells as $GL7^+$ $CD38^-$ B cells (**Figure 4A-B**). PNA labeling might be used instead of GL7[23] whereas CD38 can be replaced by one of the following markers: IgD, Bcl-6, and CD95. Alternative gating strategies for GC B cells are demonstrated in **Figure S1.** GC B cell ratio in PPs shows great variability in C57BL/6 mice. However, compared to other SLOs, PPs have significantly higher GC B cell ratio with a range of 2-10% of total B cells under steady-state conditions. Gating strategy for PP TFH cells is described as $CD19^-$ $CD4^+$ $PD\text{-}1^{hi}$ $CXCR5^+$ T cells (**Figure 4A, C**). “Zebra plot” was found to be an optimal demonstration method for TFH gating as it depicts $PD\text{-}1^{hi}$ population more discretely compared to other plot types (**Figure 4C**). TFR, a subset of TFH cells expressing Foxp3, are gated as $CD19^-$ $CD4^+$ $PD\text{-}1^{hi}$ $CXCR5^+$ $Foxp3^+$ T cells (**Figure 4D**). Like GC B cells, the TFH cell fraction also varies in unimmunized mouse individuals with a range of 10–20% of total $CD19^-$ $CD4^+$ PP lymphocytes. Details of alternative gating algorithms for TFH cells are described in **Figure 4E, F** and **Figure S1C, D.**

To avoid false positivity due to background staining and autofluorescence, isotype controls or alternative equivalent controls such as Fluorescence Minus One (FMO) should be included in the staining panel as a negative control for TFH and GC B cell markers (**Figure 4G-J**).

To optimize the conditions for PP tissue preparation, we developed a novel internally controlled experimental strategy, in which PPs were collected from one individual mouse and pooled separately depending on their anatomical origin (*e.g.*, duodenal, ileal). For performing experiments, pooled PPs were assigned to individual groups so that each experimental and control group included an equal number of PPs from each anatomical region (**Figure 5A**). By this approach, we found that collagenase-based enzymatic digestion (tested at 37.5 mg of collagenase II or IV per 25 mL of digestion mix = 1.5 mg/mL), which is commonly used for lymphocyte isolation from various mucosal tissues, significantly reduced CXCR5 expression in PP lymphocytes (**Figure 5B**), particularly in TFH cells (**Figure 5F-I**), while the expression of other surface molecules (*e.g.*, CD19, CD4) remained intact (**Figure 5C-E**). Reduction of CXCR5 detection was prominent so that the expression of CXCR5 on collagenase-treated TFH cells was almost indistinguishable from isotype control (**Figure 5F-I**). Further experiments showed that the interference level of enzymatic digestion with CXCR5 expression was dependent on the CXCR5 antibody clone used (**Figure 6A-F**). Specifically, upon collagenase II treatment, the detection capacity of CXCR5 antibody clone 2G8 was more significantly impaired, than the detection capacity of the CXCR5 antibody clone L138D7 (**Figure 6A-D**).

Enzymatic digestion reduced not only the expression of CXCR5 but also the proportion of total lymphocytes within PP cells as determined by the FSC-SSC characteristics, while a considerable fraction of cells isolated from digested PPs exhibited forward and side scatter of a higher intensity than PP lymphocytes (**Figure 7A-C).** The effects of collagenase on cell recovery occurred in a dose-dependent manner **(Figure 7A, H-J)**. Enzymatic digestion increased the cell viability **(Figure 7D, E)**. However, this benefit was not causatively linked to collagenase digestion because the cells isolated from PPs after the agitation without collagenase were favored similarly **(Figure 7F).** The detection of the nuclear transcription factor Foxp3, which is of particular interest here because it is usually assessed during TFH isolation to identify TFR cells, was improved by the agitation at 37 °C regardless of the collagenase digestion (**Figure 7G**).

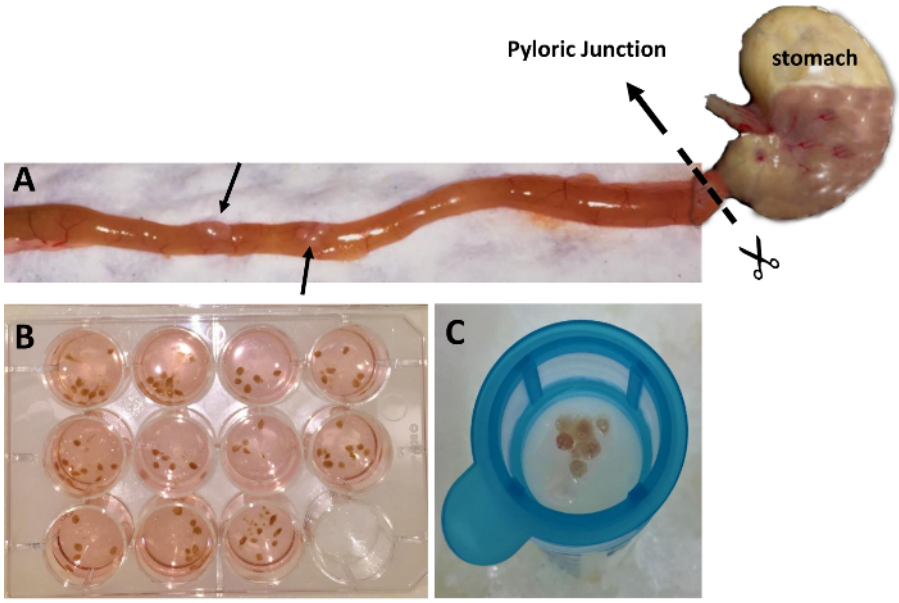

Figure 1: Macroscopic structure and anatomical distribution of murine Peyer's Patches. (**A**). An image obtained from duodenal-end of the small intestine with the stomach. Two closely-located PPs in the duodenum are indicated with black arrows. (**B**). PPs collected from eleven C57BL/6 mice were stored individually in a 12 well-plate. (**C**). Image of freshly excised mouse PPs displayed on a 40 µm cell strainer. Please click here to view a larger version of this figure.

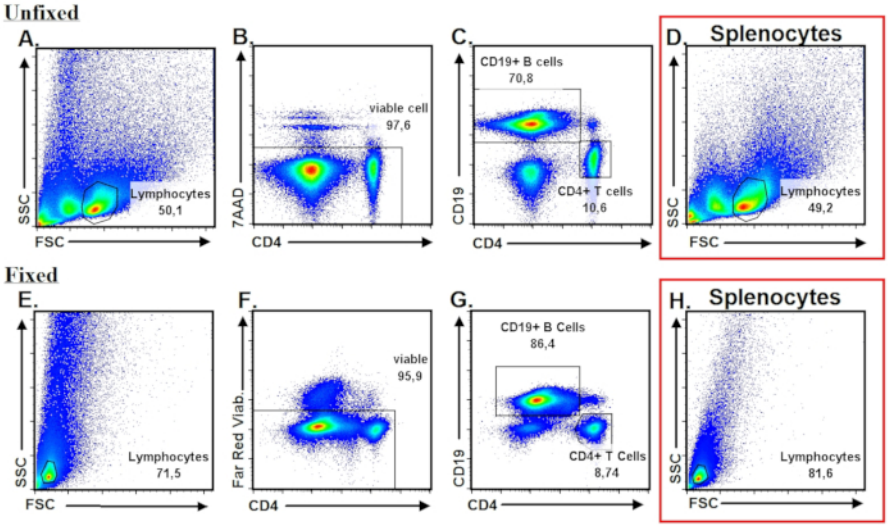

Figure 2: Flow cytometric characterization and basic gating algorithm for PP lymphocytes. (**A**). Dot plots demonstrate the distribution of freshly isolated unfixed PP lymphocytes along FSC and SSC axes which exhibit great similarity to splenocytes depicted in (**D**). (**B**). Exclusion of dead cells by means of 7AAD expression. 7AAD$^-$ cells represent live cells. (**C**). CD19 and CD4-based immunophenotyping of T and B cells among pre-gated live PP cells. (**E-G**). Representative flow analysis of fixed PP lymphocytes. (**H**). Representative flow characteristics of fixed splenocytes. Please click here to view a larger version of this figure.

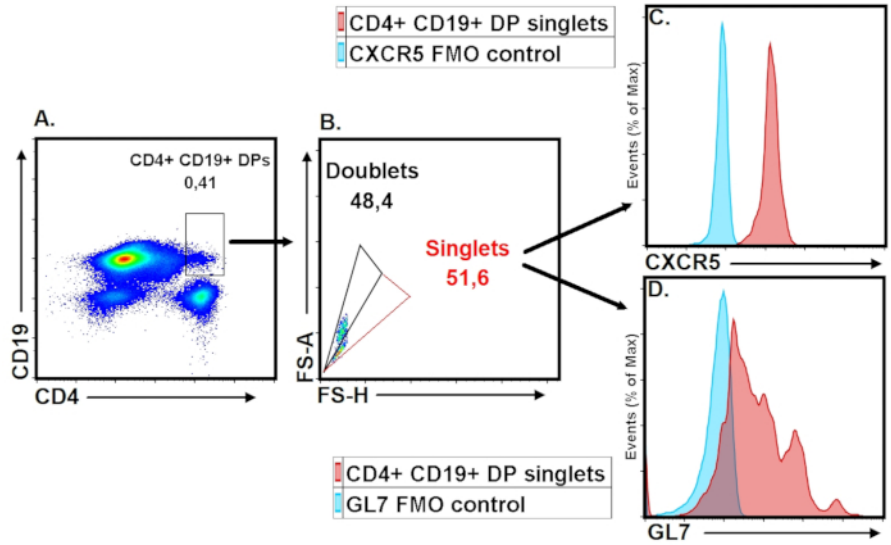

Figure 3: CD4$^+$ CD19$^+$ Double Positive (DP) cells cause false positivity in TFH and GC B cell gating. (**A**). CD4$^+$CD19$^+$ DP lymphocytes within live PP cells are demonstrated. (**B**). Separation of DP cells based on FSC characteristics as doublets and singlets. (**C**,**D**). CXCR5 and GL7 expression of DP cells are depicted in histogram plots. Please click here to view a larger version of this figure.

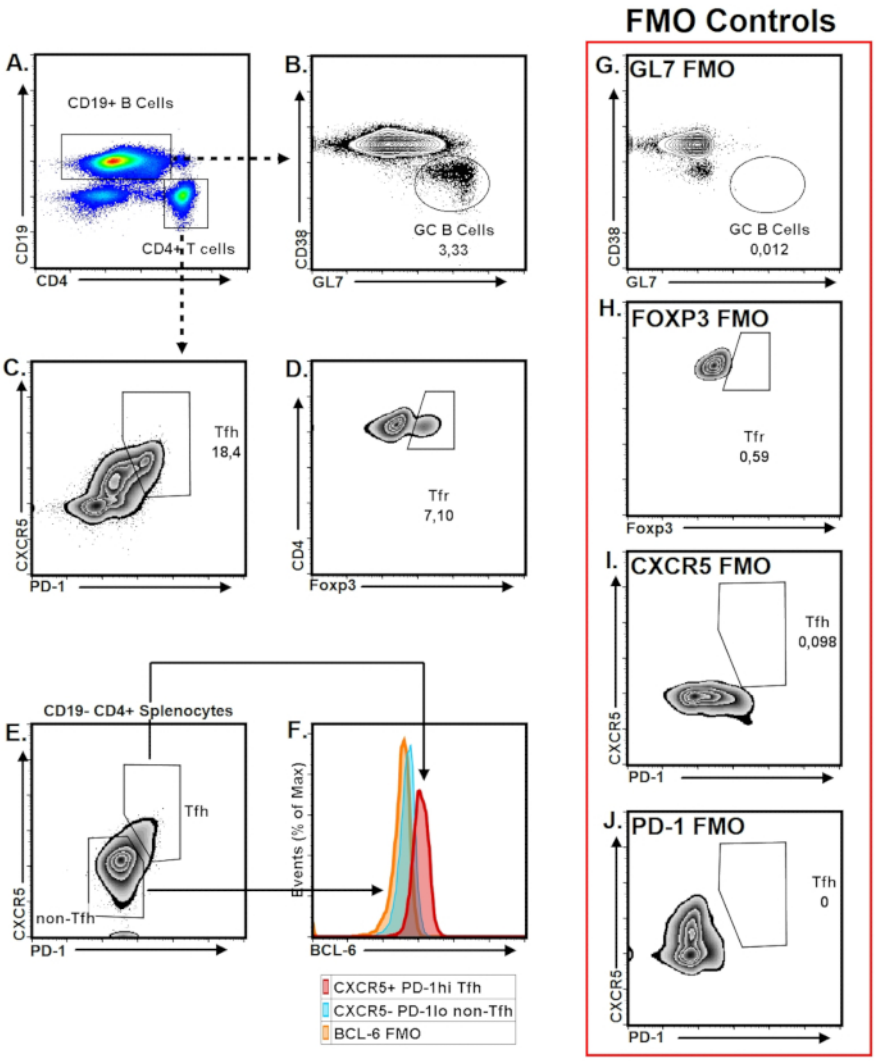

Figure 4: Representative TFH and GC B cell gating strategy. PPs were collected from a 3-month old mouse and lymphocytes were isolated as described in the Protocol section. (**A**) CD19 and CD4 labeling of live PP lymphocytes are depicted. (**B**) $CD38^{lo}$ $GL7^{hi}CD19^{+}$ B cells were gated as GC B cells. (**C**) TFH cells were gated as $CXCR5^{+}PD\text{-}1^{hi}$ $CD4^{+}$ cells. (**D**) TFR cells are a fraction of TFH cells expressing regulatory cell-specific transcription factor Foxp3 together with TFH markers and are gated as $CXCR5^{+}$ $PD\text{-}1^{hi}$ $Foxp3^{+}$ $CD4^{+}$ T cells. (**E-F**) Gating strategy for TFH surface markers confirmed in splenocytes isolated from NP-OVA-immunized mouse by means of BCL-6 expression. (**G-J**) Fluorescence Minus One (FMO) controls for key TFH-TFR and GC cell markers are depicted. Please click here to view a larger version of this figure.

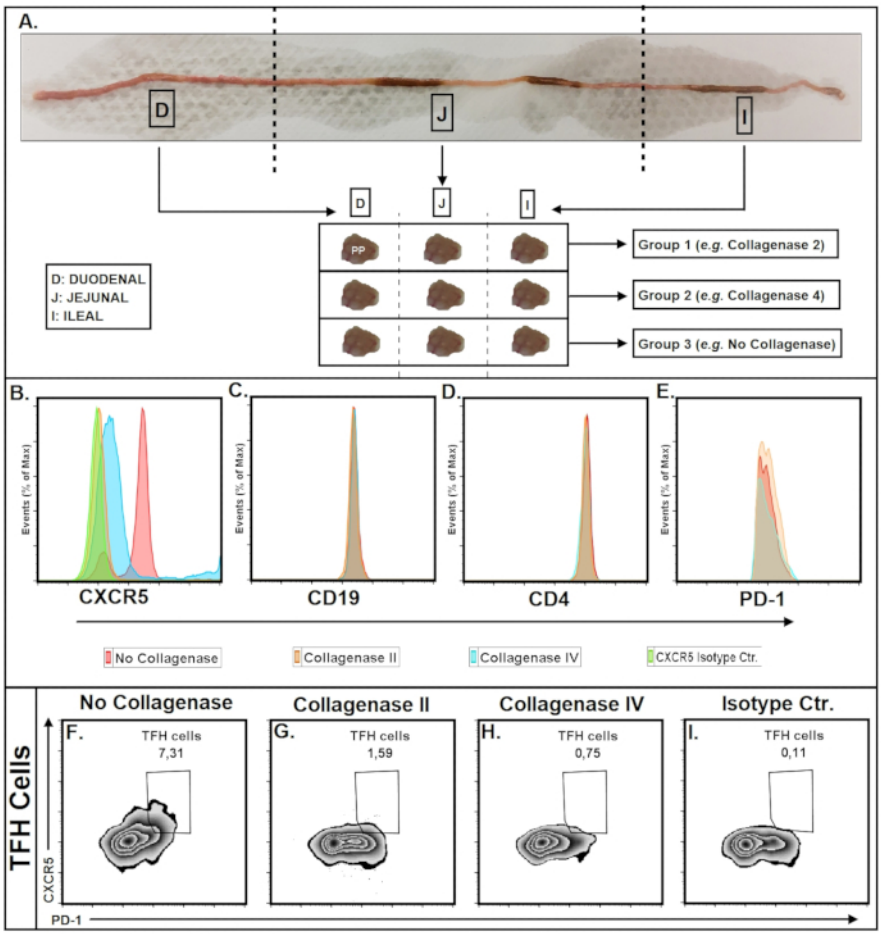

Figure 5: Collagenase-based enzymatic digestion leads to a massive reduction of CXCR5 detection. (**A**) PPs from a 2 month-old mouse located in the duodenum (≈ 1/3 proximal), jejunum (≈ 1/3 middle) and ileum (≈ 1/3 distal) were collected and pooled separately. Pooled PPs were equally distributed to the experimental groups. Enzymatic digestion with collagenase II or IV at 1.5 mg/mL concentration was performed with agitation for 10 min at 37 °C. (**B-E**) Histogram plots depicting the expression of surface molecules (CXCR5, CD19, PD-1, CD4) of the cells isolated from PPs that were subjected to collagenase-based digestion. (**F-I**) TFH gating within the collagenase-administered and control groups is demonstrated in zebra plots. Data represent three independent experiments. Please click here to view a larger version of this figure.

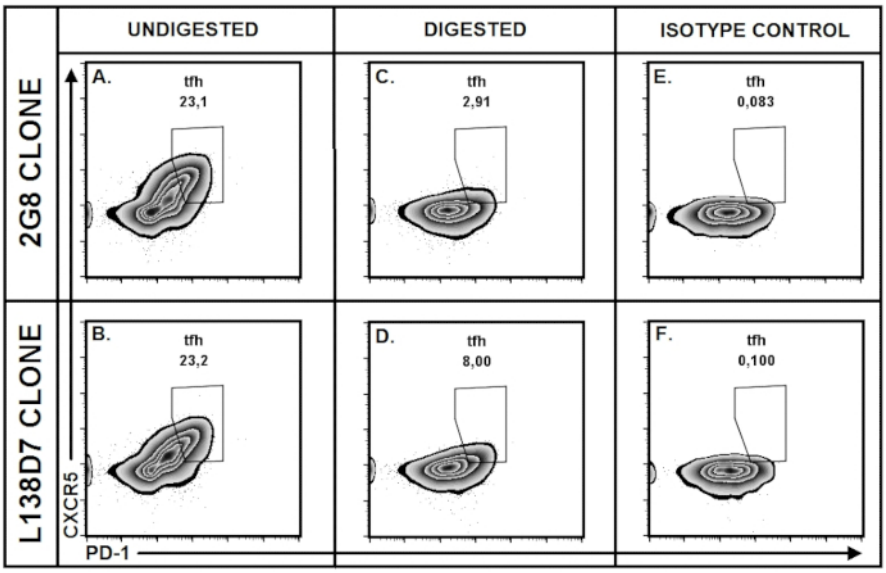

Figure 6: The effect of collagenase on CXCR5 expression showed great difference depending on the anti-CXCR5 antibody clone. PP lymphocytes collected from a 6-month-old mouse, pooled and separated into different groups regarding antibody clone used and enzymatic digestion application. (**A-F**) The proportion of TFH cells is depicted in zebra plots within pre-gated live, $CD19^{-}$ $CD4^{+}$ T cells. (**A, C** and **E)** PP cells were stained with the Biotin-conjugated anti-mouse CXCR5 antibody (2G8 clone), and Streptavidin conjugated with BV421 fluorochrome. (**B, D** and **F**) PP cells were stained with a primary conjugated anti-mouse CXCR5 antibody (L138D7 clone). (**A-B**) TFH gating plots from undigested PP lymphocytes. (**C-D**) PPs digested with collagenase II (20 mg/25 mL of digestion mix) and agitated for 10 min at 37 °C. Data represent two independent experiments. Please click here to view a larger version of this figure.

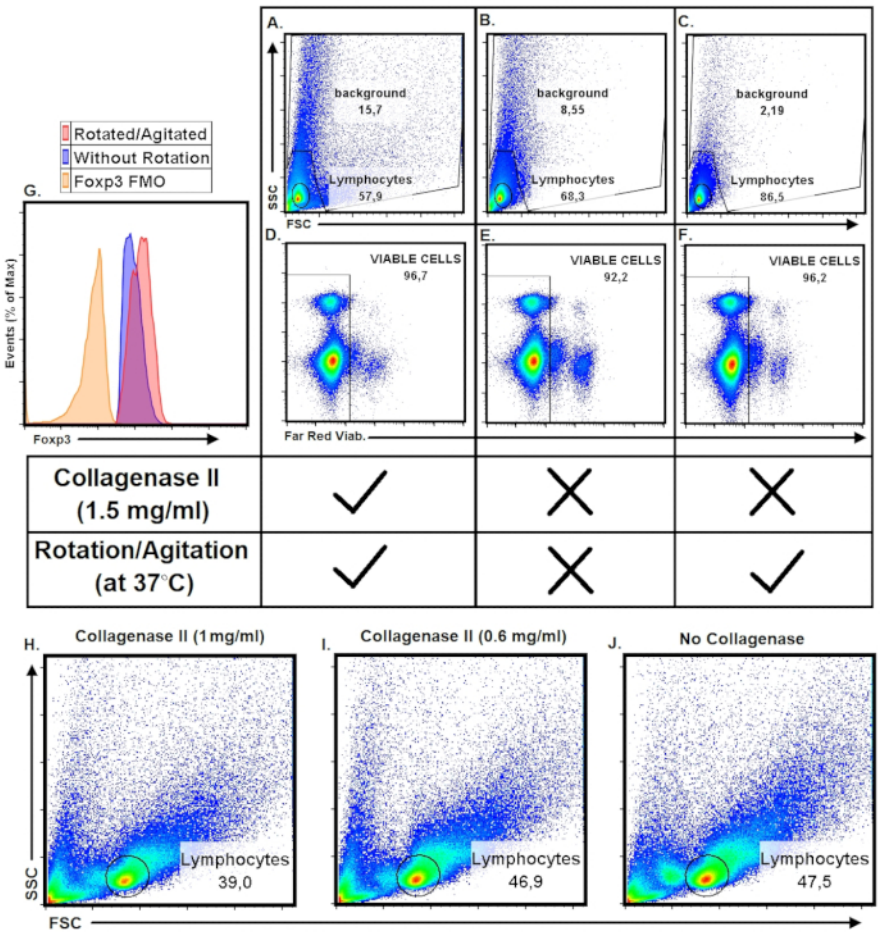

Figure 7: Collagenase-based digestion and agitation at 37 °C influence cell viability, recovery and intracellular staining efficiency. A 3 month-old C57BL/6 mouse was sacrificed; PPs were collected and pooled as described in **Figure 5A**. (**A**) After the collection of PPs, the tissues were agitated in the presence of collagenase II (37.5 mg/25 mL of digestion mix) for 10 min, FSC and SSC characteristics of fixed PP cells are depicted in (**A**) and viability staining plot is depicted in (**D**). (**B, E**) After the collection of PPs, the tissues were kept on ice without agitation or enzymatic digestion; FSC and SSC characteristics of fixed PPs cells are depicted in (**B**) and viability staining is depicted in (**E**). (**C, F**) After the collection of PPs, tissues were agitated at 125-150 rpm for 10 min at 37°C in the absence of collagenase; FSC and SSC characteristics and viability staining of fixed PP cells are depicted (**C, F**), respectively. (**G**) Comparison of Foxp3 expression in regulatory T cells isolated from agitated and unagitated PPs without collagenase administration is depicted in the histogram plot. (**H-J**) PPs collected from a 6-month old C57BL/6 mouse and were treated with different concentrations of collagenase II: 25 mg per 25 mL digestion mix, 15 mg per 25 mL digestion mix or no collagenase. FSC and SSC plots which reveal the effects of enzymatic digestion on PP cell recovery and yield are depicted. Please click here to view a larger version of this figure.

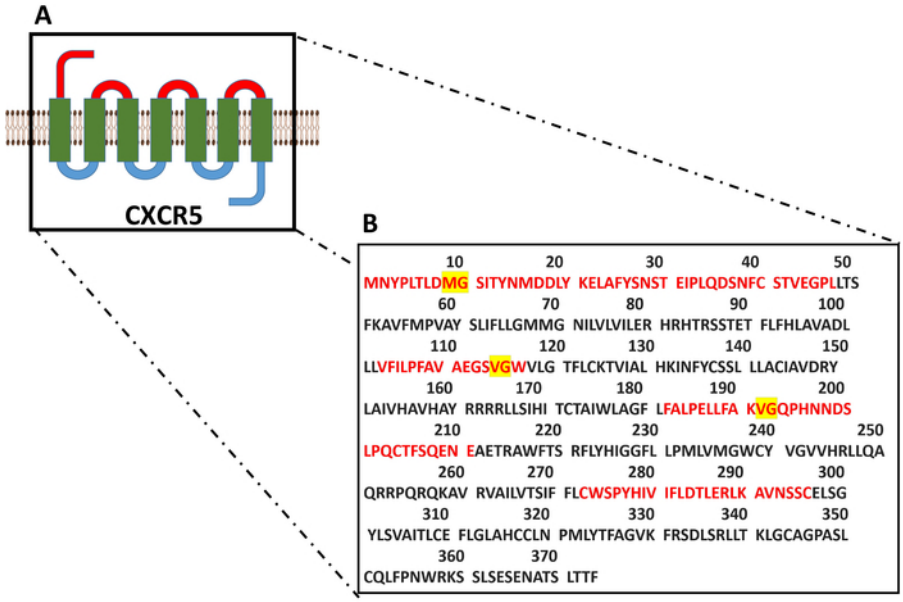

Figure 8: The molecular model and the complete amino acid sequence of CXCR5. (**A**) Seven-pass transmembrane protein structure of CXCR5 is modeled. (**B**) The complete amino acid sequence of CXCR5 is demonstrated. The sequence of extracellular regions is indicated in red and extracellular amino-acids with presumable collagenase sensitive chemical bonds are demonstrated in yellow. Please click here to view a larger version of this figure.

Antigen	Clone	Fluourochrome	Dilution
CD4	GK1.5,RM4-5	APC, PECy7, PerCpCy5.5, FITC	**1:100**
CD19	6D5	FITC, APC/Cy7	**1:100**
PD-1	J43	PE ef 610 (Texas Red)	**1:100**
ICOS	15 F9, 7E.17G9	PE	**1:100**
GL7	GL7	PerCp/Cy5.5	**1:75**
CXCR5	2G8,**L138D7***	Biotin	**1:50**
BCL-6	7D1	PE/Cy7	**1:50**
FOXP3	FJK-16	APC, PE	**1:100**
Streptavidin	-	BV421, PE	**1:100**
FixableViability Dye	-	BV 510(AQUA)	**1:1,000**
7AAD	-	PerCp/Cy5.5	**1:500**
FcBlock (CD16/32)	2.4G2	-	**1:200**

Table 1: Antibody summary. The dilutions, clones and fluorochrome conjugations for the relevant antibodies and viability dyes are indicated. The optimal dilution might vary depending on experimental conditions and lot quality of the product. Primary BV421-conjugated L138D7 clone at 1:20 dilution showed comparable CXCR5 detection capacity with the biotin-conjugated 2G8 clone at 1: 50 dilution. Therefore, primary-conjugated L138D7 can be used as alternative to biotin-conjugated 2G8 clone.

Figure Supplementary 1 (S1): Alternative gating strategies for TFH and GC B cells. (**A**) Live PP lymphocytes from a 3 month-old mouse on the C57BL/6 background are depicted. (**B-C**) GC B cells are gated as $CD38^{-}$ $GL7^{+}$ (B) and BCL-6^{+} $GL7^{+}$ B cells (C). (**D-E**) TFH cells are depicted as PD-1^{hi} $CXCR5^{+}$ (D) and as $ICOS^{+}CXCR5^{+}$ CD4+ T cells (E). Please click here to download this file.

Discussion

Here, we describe a protocol optimized for flow cytometric characterization of TFH and GC B cells. One of the major advantages of our protocol is that it enables the isolation of up to 10^7 (average 4–5 x 10^6 cells) total PP cells from a single mouse (C57BL/6 strain) without any digestive process. We observed that the total cell yield was positively correlated with the number of PPs and could be estimated from the following simple equation which is helpful for experimental planning: "total PP cell count *per* mouse = 0.5–1 x (number of excised PP *per* mouse) x 10^6". This high cell yield was complemented with enhanced cell viability (>95%). Improved cell recovery and viability allowed performing flow cytometric analysis of various lymphocyte subsets in PPs using diverse antibody staining panels in parallel.

Compared to a recent PP isolation protocol published by De Jesus *et al.*[20] and previous reports[19,21], our protocol gave considerably higher total cell yield and viability, in spite of the absence of the digestion with collagenase. Although the identification of PPs might be "tricky" for the

first-time investigators, the learning curve for this protocol is pretty steep, and if mastered, our technique allows the identification and surgical excision of PPs from the small intestine in a short time. If the desired PP number is not reached after the first attempt, we suggest repeating the PP identification step focusing on the distal and proximal end of the SI. In our practice, almost in every mouse, two closely located PPs in the duodenal end (**Figure 1A**) and at least 2–3 PPs within the last 5 cm of the ileum were detectable.

TFH staining can be more demanding than other cell subsets within the PPs, thus requiring extra attention[18]. If certain steps are missed during tissue processing and cell isolation, results might be quite misleading. Hence, we suggest researchers to pay attention to the following experimental "tips". Since key TFH and GC B cell markers such as CXCR5 and GL7 can be expressed in both B and T cells, it is critical to include a B cell marker in antibody panels to avoid false positive results due to the contaminating $CD19^{+}CD4^{+}$ DP cells[24] (**Figure 2**). Please note that gating strategies based on T cell markers only[25] will not provide sufficient exclusion of DP cells since these cells also highly express T cell markers including CD3 (data not shown) and CD4. In addition to the exclusion of DP cells, flow cytometry results should be validated and confirmed by employing appropriate negative controls (*e.g.*, isotype controls, FMOs). Not only false positivity but also misplaced TFH gate can lead to false results and conclusions. Adjustment of TFH gate could sometimes be challenging especially if TFH cell population is not abundant, thereby not appearing as a discrete population in flow cytometry. To circumvent this limitation, the addition of multiple TFH markers (*e.g.*, BCL-6, PD-1, ICOS) into antibody panel might provide alternative gating opportunities and increase accuracy[26]. For practical reasons, BCL-6 was found to be an ideal co-staining marker for alternative TFH gating as it can be used for gating GC B cells concurrently[16] (**Figure S1C**).

Furthermore, having a positive control sample containing a high TFH proportion could provide researchers good navigation for placing TFH gate correctly. In our experiments, we used PP samples from aged mice (older than 6-months) as a positive control since we have found that aging causes the enhancement of TFH cells within PPs up to 40% of total $CD4^{+}$ T cells in steady state (data not shown). We also encourage the researchers that have further interest in technical details of TFH staining to look at the methods in the published protocol book for TFH cell staining[18].

Testing experimental hypotheses in PP can be relatively challenging and might require a very high number of mice per group to reach statistical significance[21]. By taking advantage of the high cell yield of our protocol, we circumvented this obstacle with the following experimental strategies. First, we excised PPs and sorted them separately depending on their anatomical origin (*e.g.*, duodenal, jejunal and ileal). Then, we equally distributed these pooled PPs into different experimental and control groups. This internally controlled experimental strategy enabled us to minimize the inter-individual difference in mice while all cells were obtained from a single mouse.

Furthermore, variability between different intestinal compartments (*e.g.*, duodenum *vs.* ileum) -previously reported to be significant[2] — was prevented as experimental and control groups consisted from an equal number of PPs per anatomical region (**Figure 5A**)**.** By performing replicates of independent experiments using the same approach, we improved the reliability and significance of our results. Besides eliminating nonspecific variations, this methodology also helps spare mice, reagents and time.

During the development and optimization of our protocol, our results revealed that collagenase II- and IV-based digestion strikingly reduced CXCR5 expression (**Figure 5B**) while other surface molecules for detection TFH and GC B cells remained intact (**Figure 5C-E**)**.** In a recently reported JoVE protocol[19], collagenase II was shown to be very effective for lymphocyte isolation from PPs and LPs. However, collagenase II has previously been reported to have a high tryptic activity, which results in cleavage of several surface molecules. Given its surface-molecule friendly nature[27] due to the lower tryptic activity and more common usage in the literature[28,29,30], Collagenase IV had also been included in addition to collagenase II in our study and used in the concentrations as recommended in these previous reports. The use of collagenase and equivalent enzymes has been a contradictory issue in mucosal immunology due to the unwanted effects of the digestion on immune cells such as altered surface molecule expression[31,27].

It was previously reported that the use of different types of collagenase could interfere with flow cytometric CXCR5 detection within human gut[32] and tonsil samples[18]. Conversely, other studies demonstrated the isolation of TFH and GC B cells from PPs without the use of collagenases[24,33]. However, until now no comparative approach had been undertaken to assess whether the inclusion or exclusion of collagenase digestion would represent the optimal condition for isolation of CXCR5-expressing TFH cells from murine PPs. Mouse CXCR5 is a 374 amino acid long seven-pass membrane protein with relatively short extracellular regions compared to other transmembrane proteins such as CD4, CD19 that are abundantly expressed in lymphoid cells in PPs (data obtained from UniProt). In **Figure 8A-B**, a molecular model and total amino acid sequence of mouse CXCR5 are depicted with the presumed target sequences of collagenase-based digestion, which tends to dissociate chemical bonds between glycine (Gly) and neutral amino acids[34]. The seven-pass transmembrane molecular structure resulting short extracellular domains might be responsible for making CXCR5 molecule vulnerable to enzymatic digestion (**Figure 8A**). Intriguingly, we found that detection of CXCR5 expression after collagenase treatment is dependent on the antibody clone used. Although 2G8 and L138D7 clones showed similar performance in the undigested PP group, as determined by the detection of comparable TFH fractions, in the digested PP group, L138D7 clone revealed approximately 3x (≈ 9%) higher fraction of TFH cells within $CD4^{+}$ T cells than the 2G8 clone (≈ 3%) (**Figure 6**). This finding suggests that reduced CXCR5 staining might be secondary to modified three-dimensional epitope configuration by the enzymatic activity of collagenase. Our results indicate that collagenase-based digestion must be avoided during PP preparation.

The interference of collagenase dissociation with CXCR5 molecule detection was circumvented by excluding the digestion step. However, it should be noted that for some tissues such as LP, mechanical disruption is not sufficient to isolate the cells and for such tissues, enzymatic digestion would be required[19]. In the future, it will be essential to test alternative digestion conditions as well as digestion-compatible antibody clones to bypass this technical limitation for tissues requiring enzymatic digestive processes. Until then, imaging techniques such as immune fluorescence microscopy will stay as the method of choice for TFH detection in these tissues. In addition to isolating LP cells, the isolation of some hematopoietic cell subsets such as DCs and plasma cells from PPs require enzymatic digestion[35]. When employing our protocol, researchers who desire to isolate these cell subsets from PPs should include the appropriate enzymatic digestion step[20]. Possible interference of enzymatic digestion with the expression of DC markers should be taken into consideration and digestion conditions should be optimized as needed. When isolation of TFH and GC B cells is desired in addition to a cell subset that requires collagenase digestion[36], PPs collected from each mouse could be separated in two groups for processing with and without collagenase treatment in parallel panels.

The effects of collagenase on PP lymphocytes were not restricted to surface molecule expression. Our results revealed that enzymatic digestion caused a relative decrease in the lymphocyte proportion within PP cells in a dose-dependent manner (**Figure 7**). The decrease of the

lymphocyte fraction might be a consequence of collagenase-mediated release of other types of hematopoietic cell subsets such as phagocytes and DCs from PPs that are larger and more granular than lymphoid cells. It is also possible that collagenase digestion mediated cell release from neighboring LP and intraepithelial compartments could contribute to the change of FSC-SSC profile. This cell contamination from other gut compartments might also cause interference in the flow analysis of PP lymphocytes. On that basis, to maximize cell purity, we also avoid the addition of reagents such as EDTA or DTT that are widely used to extract epithelial cells and mucus[20], keeping tissue preparation conditions as physiologic and unmanipulated as possible. Despite these adverse effects of enzymatic digestion, beneficial effects on PP lymphocytes were also discovered such as improvement of intracellular staining and cell viability (**Figure 7D-F, G**). However, further analyses revealed that these effects were attributed to the agitation process at 37 °C independently of enzymatic digestion because cell viability and intracellular Foxp3 staining were favored to a comparable extent when cells were agitated in the absence of collagenase. Mechanistically, the beneficial effect of agitation might be due to the improved removal of intestinal content and mucus from PPs.

In summary, we have described a streamlined protocol for the isolation of lymphocytes from PPs. Isolated cells can be stained for flow cytometric characterization of several cell subsets or can be subjected to cell sorting and subsequently employed in various *in vitro* and *in vivo* functional assays.

Disclosures

No conflicts of interest declared.

Acknowledgements

We would like to thank Laura Strauss and Peter Sage for helpful discussions and support with flow cytometry analyses.

References

1. van den Berg, T. K., & van der Schoot, C. E. Innate immune 'self' recognition: a role for CD47-SIRPα interactions in hematopoietic stem cell transplantation. *Trends in Immunology.* **29** (5)**,** 203-206 (2008).
2. Mowat, A. M., & Agace, W. W. Regional specialization within the intestinal immune system. *Nature Reviews Immunology* .**14** (10)**,** 667-685 (2014).
3. Reboldi, A., & Cyster, J. G. Peyer's patches: Organizing B-cell responses at the intestinal frontier. *Immunological Reviews.* **271** (1)**,** 230-245 (2016).
4. Heel, K. A., McCauley, R. D., Papadimitriou, J. M., & Hall, J. C. Review: Peyer's patches. *Journal of Gastroenterology and Hepatology.* **12** (2)**,** 122-136 (1997).
5. Fagarasan, S., Kinoshita, K., Muramatsu, M., Ikuta, K., & Honjo, T. In situ class switching and differentiation to IgA-producing cells in the gut lamina propria. *Nature.* **413** (6856)**,** 639-643 (2001).
6. Hopkins, S. A., Niedergang, F., Corthesy-Theulaz, I. E., & Kraehenbuhl, J. P. A recombinant Salmonella typhimurium vaccine strain is taken up and survives within murine Peyer's patch dendritic cells. *Cellular Microbiology.* **2** (1)**,** 59-68 (2000).
7. Shreedhar, V. K., Kelsall, B. L., & Neutra, M. R. Cholera toxin induces migration of dendritic cells from the subepithelial dome region to T- and B-cell areas of Peyer's patches. *Infection and Immunity.* **71** (1)**,** 504-509 (2003).
8. Sato, A., & Iwasaki, A. Peyer's patch dendritic cells as regulators of mucosal adaptive immunity. *Cellular and Molecular Life Sciences.* **62** (12)**,** 1333-1338 (2005).
9. Bemark, M., Boysen, P., & Lycke, N. Y. Induction of gut IgA production through T cell-dependent and T cell-independent pathways. *Annals of the New York Academy of Sciences.* **1247** (1)**,** 97-116 (2012).
10. Fagarasan, S., Kawamoto, S., Kanagawa, O., & Suzuki, K. Adaptive Immune Regulation in the Gut: T Cell-Dependent and T Cell-Independent IgA Synthesis. *Annual Review of Immunology.* **28,** 243-273 (2010).
11. Hase, K. *et al.* Uptake through glycoprotein 2 of FimH + bacteria by M cells initiates mucosal immune response. *Nature.* **462** (7270)**,** 226-230 (2009).
12. Wu, H. *et al.* An Inhibitory Role for the Transcription Factor Stat3 in Controlling IL-4 and Bcl6 Expression in Follicular Helper T Cells. *Journal of Immunology.* **195** (5)**,** 2080-2089 (2015).
13. Vinuesa, C. G., Tangye, S. G., Moser, B., & Mackay, C. R. Follicular B helper T cells in antibody responses and autoimmunity. *Nature Reviews Immunology.* **5** (11)**,** 853-865 (2005).
14. Victora, G. D., & Nussenzweig, M. C. Germinal Centers. *Annual Review of Immunology.* **30,** 429-457 (2012).
15. Vaeth, M. *et al.* Store-Operated Ca2+Entry in Follicular T Cells Controls Humoral Immune Responses and Autoimmunity. *Immunity.* **44** (6)**,** 1350-1364 (2016).
16. Meli, A. P. *et al.* The Integrin LFA-1 Controls T Follicular Helper Cell Generation and Maintenance. *Immunity.* **45** (4)**,** 831-846 (2016).
17. Fu, W. *et al.* Deficiency in T follicular regulatory cells promotes autoimmunity. *Journal of Experimental Medicine.* **215** (3), 815-825 (2018).
18. Espéli, M., & Walker, J. M. *T follicular helper cells - Methods and Protocols.* (2015).
19. Couter, C. J., & Surana, N. K. Isolation and Flow Cytometric Characterization of Murine Small Intestinal Lymphocytes. *Journal of Visual Experiments.* (111), e54114 (2016).
20. De Jesus, M., Ahlawat, S., & Mantis, N. J. Isolating And Immunostaining Lymphocytes and Dendritic Cells from Murine Peyer's Patches. *Journal of Visual Experiments.* (73):e50167. (2013).
21. Pastori, C. and Lopalco, L. Isolation and in vitro Activation of Mouse Peyer's Patch Cells from Small Intestine Tissue. *Bio-protocol.* **4** (21): e1282. (2014).
22. Fukuda, S., Hase, K., & Ohno, H. Application of a Mouse Ligated Peyer's Patch Intestinal Loop Assay to Evaluate Bacterial Uptake by M cells. *Journal of Visual Experiments.* (58), pii: 3225. (2011).
23. Naito, Y. *et al.* Germinal Center Marker GL7 Probes Activation-Dependent Repression of N-Glycolylneuraminic Acid, a Sialic Acid Species Involved in the Negative Modulation of B-Cell Activation. *Molecular and Cellular Biology.* **27** (8), 3008-3022 (2007).

24. Bollig, N. *et al.* Transcription factor {IRF4} determines germinal center formation through follicular T-helper cell differentiation. *Proceedings of the National Academy of Science of U. S. A.* **109** (22)**,** 8664-8669 (2012).
25. Pérez-Mazliah, D. *et al.* Follicular Helper T Cells are Essential for the Elimination of Plasmodium Infection. *EBioMedicine.* **24,** 216-230 (2017).
26. Sage, P. T., & Sharpe, A. H. T follicular regulatory cells in the regulation of B cell responses. *Trends Immunology.* **36** (7)**,** 410-418 (2015).
27. Van Damme, N. *et al.* Chemical agents and enzymes used for the extraction of gut lymphocytes influence flow cytometric detection of T cell surface markers. *Journal of Immunological Methods.* **236** (1-2)**,** 27-35 (2000).
28. Meenan, J. *et al.* Altered expression of alpha 4 beta 7, a gut homing integrin, by circulating and mucosal T cells in colonic mucosal inflammation. *Gut.* **40** (2)**,** 241-246 (1997).
29. Cao, A. T. *et al.* Interleukin (IL) -21 promotes intestinal IgA response to microbiota. *Mucosal Immunology.* **8 (5),** 1072-1082 (2015).
30. Wei, J. *et al.* Autophagy enforces functional integrity of regulatory T cells by coupling environmental cues and metabolic homeostasis. *Nature Immunology.* **17** (3)**,** 277-285 (2016).
31. Autengruber, A., Gereke, M., Hansen, G., Hennig, C., & Bruder, D. Impact of enzymatic tissue disintegration on the level of surface molecule expression and immune cell function. *European Journal of Microbiology & Immunology.* **2** (2)**,** 112-120 (2012).
32. Trapecar, M. *et al.* An Optimized and Validated Method for Isolation and Characterization of Lymphocytes from HIV+ Human Gut Biopsies. *AIDS Research and Human Retroviruses.* **33 (S1),** S-31-S-39 (2017).
33. Bergqvist, P., Gardby, E., Stensson, A., Bemark, M., & Lycke, N. Y. Gut IgA Class Switch Recombination in the Absence of CD40 Does Not Occur in the Lamina Propria and Is Independent of Germinal Centers. *Journal of Immunology.* **177** (11)**,** 7772-7783 (2006).
34. Keil, B., Gilles, A. M., Lecroisey, A., Hurion, N., & Tong, N. T. Specificity of collagenase from Achromobacter iophagus. *FEBS Letters.* **56** (2)**,** 292-296 (1975).
35. Mora, J. R. *et al.* Selective imprinting of gut-homing T cells by Peyer's patch dendritic cells. *Nature.* **424** (6944)**,** 88-93 (2003).
36. Reboldi, A. *et al.* Mucosal immunology: IgA production requires B cell interaction with subepithelial dendritic cells in Peyer's patches. *Science.* **352** (6287) (2016).

